ARTICLE

Size and Dynamics of Caveolae Studied Using Nanoparticles in Living Endothelial Cells

Zhenjia Wang, Chinnaswamy Tiruppathi, Richard D. Minshall, and Asrar B. Malik*

Department of Pharmacology, College of Medicine, University of Illinois, Chicago, Illinois 60612

ABSTRACT Caveolae are plasma membrane invaginations prominent in all endothelial cells lining blood vessels. Caveolae characteristically bud to form free cytoplasmic vesicles capable of transporting carrier proteins such as albumin through the cell. However, caveolae size distribution and dynamics in living endothelial cells and ability of caveolae to internalize nanoparticles are not well understood. We demonstrate here the design of a dual-color nanoparticle pair to measure noninvasively caveolae size and dynamics. First, we coated nanoparticles with BSA (bovine serum albumin) to address whether albumin promoted their delivery. Albumin has been shown to bind to protein on endothelial cell surface localized in caveolae and activate albumin endocytosis. Imaging of BSA-coated nanoparticles varying from 20 to 100 nm in diameter in endothelial cells demonstrated that caveolae-mediated nanoparticle uptake was dependent on albumin coating of particles. We also showed that caveolae could accommodate up to 100 nm diameter nanoparticles, a size larger than the diameter of typical caveolae, suggesting compliant property of caveolae. Together, our results show the feasibility of tracking multicolored nanoparticles in living endothelial cells and potential usefulness for designing therapeutic nanoparticle cargo to cross the limiting vessel wall endothelial barrier.

KEYWORDS: endothelial cells · caveola size · assembly dynamics of caveolae · dual-color nanoparticle pairs · super-resolution optical microscopy · bioconjugated nanoparticles · uptake of nanoparticles

Caveolae are membrane invaginations 60−80 nm in diameter typically with a 10−50 nm diameter neck as measured by scanning electron microscopy.[1,2] They are present in many cell types, but they are particularly abundant in the vessel wall lining monolayer of endothelial cells.[3,4] Caveolae are formed as the result of oligomerization of caveolin-1 and -2 proteins, which is needed for development of the membrane curvature, and caveolae are involved (by as yet poorly understood mechanism) in mediating endocytosis[5−7] as well as transcytosis of antibodies[8] and albumin[9] across the vascular endothelial barrier. Caveolae-mediated endocytosis is activated by Src kinase-induced phosphorylation of caveolin-1 and dynamin, the GTPase found at caveolar necks.[10−12] Caveolae assembly dynamics and size distribution have not been optically measured in living endothelial cells chiefly because these structures are much smaller than the optical diffraction limit. However, recent advances in super-resolution optical microscopy have made it possible to visualize single fluorescent molecules or nanoparticles at spatial resolution below the optical diffraction limit.[13−19] In this context, Huang *et al.*[19] used three-dimensional high-resolution imaging by stochastic optical reconstruction microscopy (STORM) to visualize the morphology of clathrin-coated pits, endocytic structures of the approximately same size as caveolae.

Here we have developed a methodology employing a dual-color nanoparticle pair to measure caveolae size distribution and assembly dynamics in living endothelial cells. An advantage of utilizing nanoparticles and studying their movement *via* caveolae in endothelial cells is that they can be made of any size and shape and exhibit optical properties such as a wide range of fluorescence spectra and have the ability to link therapeutic antibodies and other proteins.[20] Nanoparticle size can be varied from 5 to 100 nm,[21] and fluorescent polymer nanoparticles are nearly 100 times brighter and 2−3 orders of magnitude more stable against photobleaching than organic dyes and fluorescent proteins.[22,23] These properties of nanoparticles allow visualization and tracking of individual particles in cells. Moreover, understanding nanoparticle internalization by caveolae has a practical value since therapeutic antibodies and other proteins[20] can be linked to nanoparticles, and thus it becomes important to define mechanisms of nanoparticle transit in endothelial cells. Our studies were based on the premise that measurement of caveolar size, caveolae-meditated endocytosis, and trafficking is needed to en-

*Address correspondence to abmalik@uic.edu.

Received for review September 14, 2009 and accepted November 10, 2009.

Published online November 17, 2009. 10.1021/nn9012274

able the use of caveolae for the optimal delivery of nanoparticles[24−26] into and across the vascular endothelial barrier.

RESULTS AND DISCUSSION

Albumin Coating of Nanoparticles Promotes Their Internalization by Caveolae. We made albumin-coated nanoparticles of different sizes and studied their internalization and trafficking properties in cultured endothelial cells. Bovine serum albumin (BSA) was used because all studies were made in bovine endothelial cells. Albumin binds to the albumin binding protein, gp60, localized on the caveolar plasma membrane and thereby activates caveolae-mediated albumin endocytosis and transcytosis in endothelial cells.[27,28] We conjugated BSA to the nanoparticle surface as described (see Materials and Methods). BSA binding was evident both by absorption spectra and imaging of single nanoparticles conjugated by fluorescein-labeled BSA (details in Figure S1-3 in the Supporting Information). We observed by confocal imaging the internalization BSA-coated nanoparticles in endothelial cells (Figure 1A). Three-dimensional images of nanoparticles with sizes of 20, 40, and 100 nm in cells showed that all sizes in fact transited to the basolateral aspect of endothelial cells within 10 min, indicating an efficient mechanism of transcytosis (Figure S4 in Supporting Information).

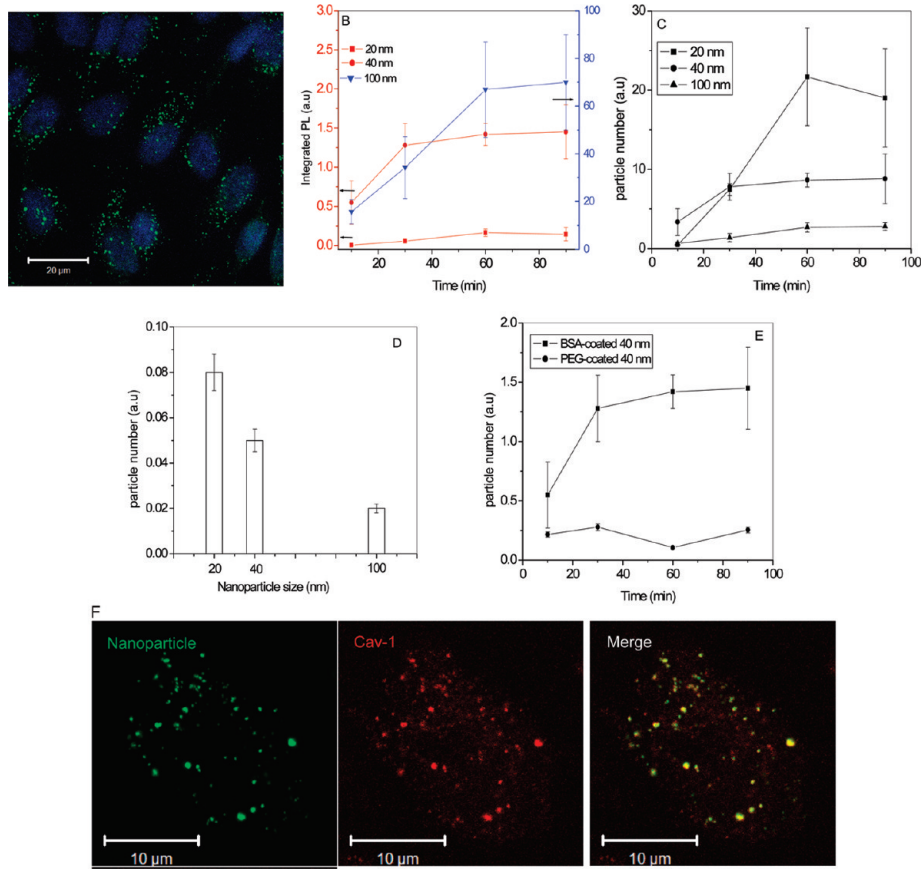

Figure 1. Uptake of albumin-coated fluorescent nanoparticles by caveolae in endothelial cells. (A) Uptake of BSA-coated nanoparticles with diameters of 20 nm incubated with bovine lung microvascular endothelial cells (BLMVEC) for 30 min. Green punctates represent nanoparticles in cells, and blue areas show nuclei stained by DAPI. (B) Photoluminescence (PL) intensity of BSA-coated nanoparticles internalized in endothelial cells as measured by fluorescence microscopy was quantified using ImageJ software (details in Supporting Information). (C) Time course of nanoparticle number of different-sized nanoparticles internalized by cells. Data in Figure 1B are normalized on the basis of size dependence of PL intensity and number of BSA molecules/nanoparticle. (D) Size-dependent uptake of nanoparticles coated with the same number of BSA molecules per different-sized particle. Nanoparticles were incubated with endothelial cells for 45 min. (E) Time-dependent uptake of two types of 40 nm nanoparticles coated with BSA (■) and PEG (●). (F) Co-localization of BSA-coated 100 nm nanoparticles with caveolin-1. *X*−*Y* projection of 3D confocal image of 100 nm BSA-coated nanoparticles is in green, and caveolin-1 immunostaining is in red. Seventy percent of nanoparticles display a caveolin-1 signal. Nanoparticles were incubated with cells for 30 min.

We next compared the uptake of albumin-coated nanoparticles of the three sizes. We imaged all nanoparticles internalized in cells using the 20× objective at several cell locations and obtained the integrated photoluminescence (PL) intensity using ImageJ software (Figure S5 in Supporting Information). The results (Figure 1B) showed that uptake of nanoparticles of all sizes was time-dependent and was saturated within 60 min. The larger nanoparticles contained more fluorescent dye and had more BSA molecules conjugated per particle. Figure 1C shows results of normalization of Figure 1B data on the basis number of internalized nanoparticle per BSA coated on a particle. These results show that the uptake of 20 and 40 nm nanoparticles was 5−10 times greater than that of 100 nm particles. Conjugation of the same number of BSA molecules per particle demonstrated clear size-dependent uptake of nanoparticles facilitated with albumin coating (Figure 1D), consistent with the normalized data (Figure 1C). We further addressed whether BSA was required to activate endocytosis of nanoparticles by comparing uptake of BSA-coated to PEG-coated nanoparticles (Figure 1E). The result shows that albumin coating of nanoparticles is a crucial determinant of particle uptake in endothelial cells.

To query the role of caveolae in mediating BSA-coated nanoparticle internalization, we investigated the pattern of co-localization of caveolin-1 and nanoparticles based on the fact that caveolin-1 is a scaffold protein associated with caveolae.[3,4] Results of immunofluorecence microscopy (Figure 1F) showed that ~70% of the BSA-coated nanoparticles co-localized with caveolin-1-positive structures, suggesting that a

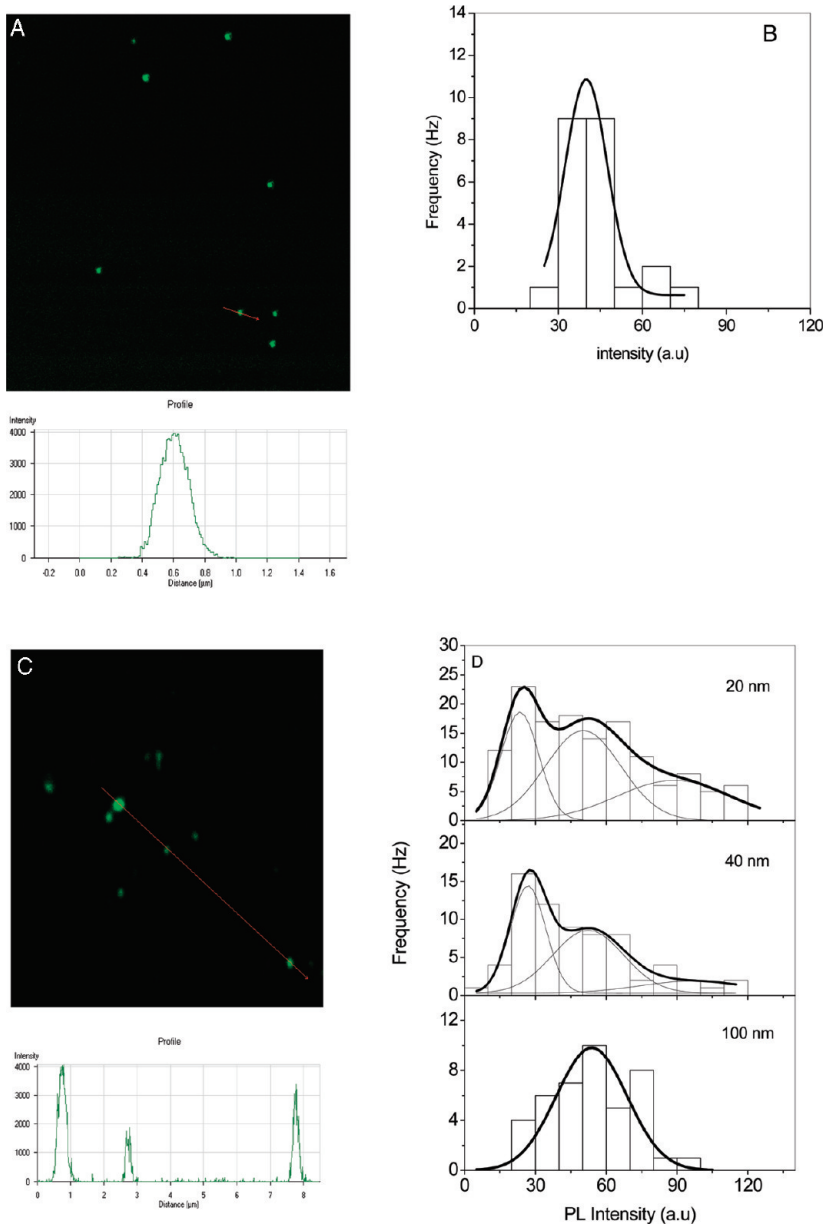

Figure 2. Multi-nanoparticle uptake by single caveolae in endothelial cells. (A) Confocal imaging of individual nanoparticles as assessed by spreading the fluorescent BSA-coated nanoparticles on a coverslip. Images show individual 40 nm nanoparticles (top), and image size profile of a single nanoparticle is in optical diffraction limit (300 nm in diameter) (bottom). (B) Histogram of fluorescent intensities from individual spots showing a narrow Gaussian distribution. (C) Image of 20 nm BSA-coated nanoparticles internalized by endothelial cells where three spots show similar quantal increases in PL intensity (bottom). The spot sizes are in optical diffraction limit. (D) Histograms of PL intensities of individual spots, indicating that a single caveola internalizes multiple 20 nm nanoparticles compared to the larger particles. The figure shows results of 20, 40, and 100 nm particles from top to bottom. Histograms were fitted by multiple Gaussian functions, and peak intensity of each Gaussian profile was shown to increase by quantal size in the case of 20 and 40 nm particles.

major portion of BSA-coated nanoparticles was internalized by caveolae.

Caveolae Can Accommodate Multiple Nanoparticles. A single caveola is in the range from 60 to 80 nm in diameter based on electron microscopic measurements.[1,2] Total internal reflection fluorescence microscopy (TIRFM) showed that multiple caveolae can assemble to form the so-called caveosomes.[12] We next addressed the question whether a single caveola containing more than one particle can be visualized by a quantal PL increase of the nanoparticle if each particle has a similar PL intensity. To address this question, we first investigated the detection capability of individual nanoparticles, homogeneity of fluorescence of a single particle, and whether individual nanoparticles remain disaggegated after coating with BSA to ensure the delivery of a single nanoparticle to cells. Figure 2A shows isolated spots of fluorescence using a dilute suspension of BSA-coated 40 nm nanoparticles dispersed on a coverslip. The fluorescence spots are in the range of the optical diffraction limit. We also observed no aggregation of particles. A histogram of fluorescence intensity of individual spots showed a narrow Gaussian distribution (Figure 2B), indicating that each spot contained a single particle and each particle exhibited similar fluorescence intensity. The BSA-coated nanoparticles internalized in endothelial cells, however, showed a broad range of fluorescent intensities (Figure 2C). The PL intensity from three spots in a cell exhibited a quantal increase (shown in Figure 2C), indicating that a single caveola can contain more than one 20 nm nanoparticle. We integrated the PL intensity on single fluorescent spots whose size was in the optical diffraction limit and statistically analyzed the PL distributions (Figure 2D). These results showed that fluorescent spots exhibited a broad range of PL intensities in the case of 20 or 40 nm nanoparticles. After fitting the histograms, we noted that there were three Gaussian profiles for 20 nm nanoparticles, two profiles for 40 nm nanoparticles, and one profile for 100 nm nanoparticles. PL intensity at each Gaussian peak in the case of 20 or 40 nm particles increased by a quantal number. We conclude from this analysis that one caveola or caveosome can contain up to three 20 nm nanoparticles, two 40 nm nanoparticles, and surprisingly only one 100 nn nanoparticle, indicating that (i) size, in addition to albumin coating, is a key determinant of nanoparticle uptake by caveolae and (ii) a caveola can accommodate a particle larger than the size range of caveolae measured using TEM.

Measurement of Caveolae Size Using a Dual-Color Nanoparticle Pair. We next addressed the question of caveolae size using dual-colored nanoparticle pairs. We first determined whether a single caveola is distinguishable from the larger caveosome. As fluorescent spots of caveolae

and caveosomes are less than or close to optical diffraction limit, we cannot differentiate these organelles by counting the particle number as in Figure 2D. Thus, we developed a nanoruler made of a dual-color nanoparticle pair to overcome the detection barrier. Figure 3A shows the concept of the ruler by comparing a dual-color nanoparticle pair to a single-color pair. The dual-color nanoparticle pair can be optically distinguished since the color-coded separate diffraction limit spots are recognizable. Locating each color-coded diffraction spot provides a measure of the distance between the two nanoparticles that is less than the optical diffraction limit (*i.e.*, less than a half of wavelength). Figure 3B shows results of internalization of a mixture of BSA-coated 40 nm green and 40 nm red fluorescent nanoparticles in endothelial cells. We observed three distinct populations of fluorescent spots, green, red, and yellow, representing green and red nanoparticles and co-localization of red and green, respectively. Zooming-in on the merged yellow spots showed a spatial separation between the centers of diffraction spots of green and red nanoparticles (Figure 3B); in this example, the separation distance was 80 nm. As it is possible that a separation can be caused by error in optical measurement such as color aberration of objectives and mis-collimation of two excitation wavelengths (at 488 and 543 nm), we measured co-localization of excitation laser wavelengths at 488 and 543 nm using single nanoparticles, which fluoresce at both excitation wavelengths (Figure S6 in Supporting Information). We observed greater than 95% co-localization of red and green spots, indicating that the two laser beams have the same optical focus. In addition, we delivered a mixture of 40 nm red and 40 nm green fluorescent nanoparticles that can both be excited using a single wavelength at 488 nm and observed similar results as in Figure 3B. Next, to measure sizes of caveolae and caveosomes, we combined the different sizes of dual-color nanoparticle pairs internalized in endothelial cells and determined caveolae and caveosome linear size by incorporating the separation distance of the two-color spots of nanoparticles. These results showed the size distribution of caveolae and caveosomes in living endothelial cells (Figure 3C). The histograms were fitted by two Gaussian profiles in the pairs of 20 nm (green) and 40 nm (red) and pairs of 40 nm (green) and 40 nm (red). This finding pointed to the presence of vesicles of 100 nm, which are in the range of typical caveolae. Also, there were a number of larger structures of ~250 nm, which may represent caveosomes. Pairs of 100 nm (green) and 40 nm (red) measured even larger intracellular vesicle structures, which

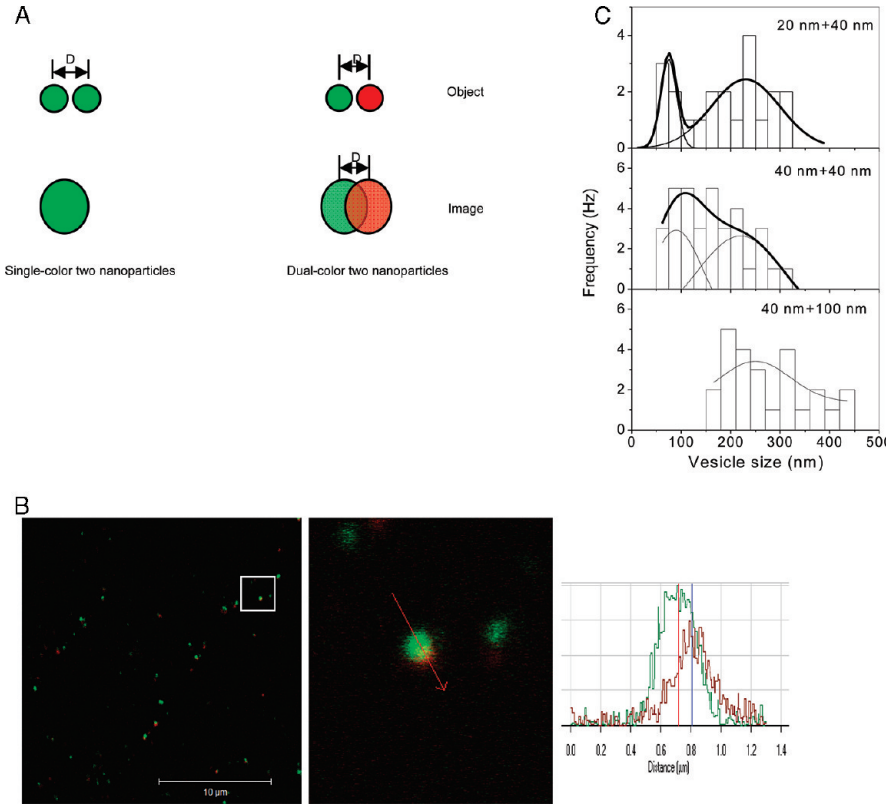

Figure 3. Two populations of caveolae in endothelial cells detected by a nanoruler made of a dual-color nanoparticle pair. (A) Concept of a nanoruler using a dual-color nanoparticle pair. Left: Two nanoparticles (indicated as two green dots) with single-color (similar fluorescence spectrum) are separated in a distance of *D* less than a half of emission wavelength. The use of separate detectors will measure the same fluorescent profile in the optical diffraction limit (indicated as a large green spot in an image plane). Right: Two nanoparticles having different colors (indicated as red and green dots). Red and green nanoparticles detected using appropriate filters will show two diffraction spots in the image (as indicated by red and green spots). Measuring the distance between centers of diffraction spots provides the linear distance between particles that is less than the optical diffraction limit. (B) Merged images of dual-color pairs of 40 nm BSA-coated nanoparticles in endothelial cells (green particle emission at 515 nm and red particle emission at 605 nm). The image of the nanoparticles was acquired at 488 nm for green and 543 nm for red. Left: Image showing three types of fluorescent spots; red, green, and yellow representing red particles, green particles, and co-localization of red and green nanoparticles (scale bar = 10 μm). Middle: Magnified view of the white-boxed region in the left image showing co-localization of red and green nanoparticles. Right: Image size profile of red and green nanoparticles showing the separation between two nanoparticles, and the separation is obtained by measuring the distance between centers of diffraction images of red and green nanoparticles; for example, in this case, the separation is 80 nm less than the diffraction limit. (C) Histograms of caveola sizes in cells measured by using a nanoruler combining different sizes of red and green nanoparticles. Mixture of red and green nanoparticles was incubated with cells for 30 min. Top: 20 nm (green) + 40 nm (red). Middle: 40 nm (green) + 40 nm (red). Bottom: 100 nm (green) + 40 nm (red). Histograms are fitted by one or two Gaussian distributions. Results show two sizes of caveola; 100 nm of size corresponding to single caveolae, and 250 nm indicating aggregates of caveolae, so-called caveosomes.

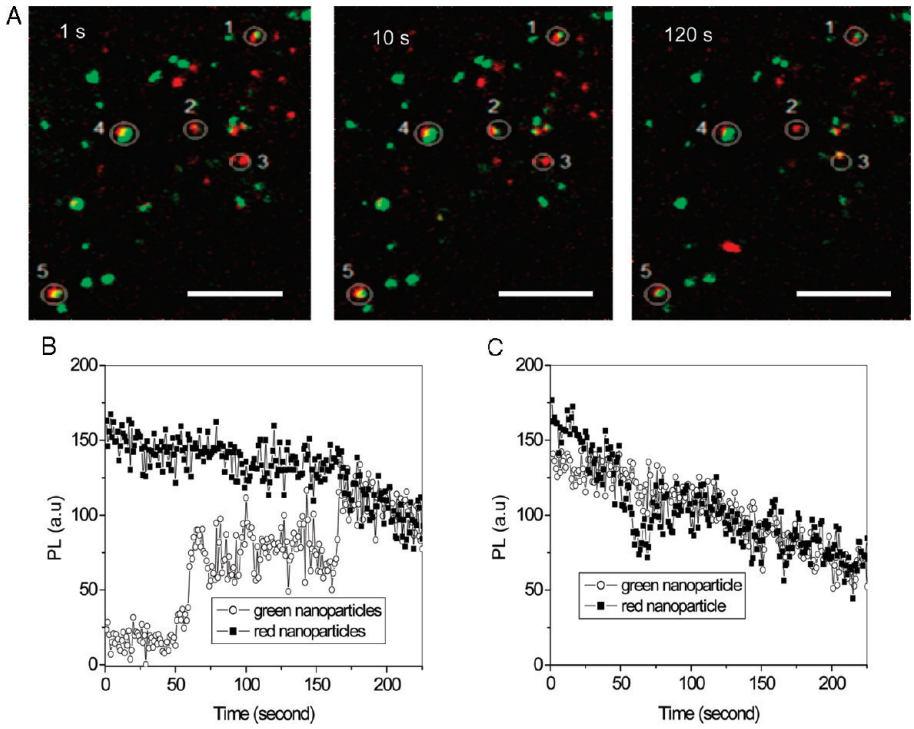

Figure 4. Tracking of dual-color nanoparticle pairs in living endothelial cells. (A) Snapshots of confocal imaging in the simultaneous dual-color detection using LSM 510 meta at a fast scanning rate (scale bar = 5 μm). The imaging plane is in the cells, and images were acquired after 10 min of adding a mixture of red and green BSA-coated nanoparticles (40 nm). The movie shows that at least two nanoparticles share a single caveola/caveosome; spots 1, 2, and 3 are associated with a single caveolae due to local and long-distance movement; spot 4 and 5 are associated with caveosomes due to their immobility (movie in Supporting Information). (B) Time-lapse of spot 3 shows a multiple step in which two caveolae fuse to form a caveosome. (C) Time-lapse of spot 5 shows excellent PL correlation between red and green spots, indicating that in this case the nanoparticles always share the same caveosome compartment.

may represent even larger caveosomes. The results are, in general, consistent with caveolae and caveosome sizes measured by electron microscopy.[29] Moreover, they show the utility of such as nanoruler made of a dual-color-coded nanoparticle pair to measure size of organelles smaller than optical diffraction limit.

Caveolae Dynamics in Living Endothelial Cells. To assess the assembly dynamics of caveolae, we simultaneously tracked dual-color nanoparticles internalized by cells. Figure 4A shows snapshots of the movie (Figure S7 in Supporting Information), indicating there are two types of patterns of co-localization of nanoparticles: one is highly motile (spots 1, 2, and 3) and the other is immotile (spots 4 and 5). In the control experiment of the two-color nanoparticle mixture dispersed in water/PEG (MW 400), we did not observe such a co-localization of red and green nanoparticles. Thus, the change in co-localization spots reflects trafficking of caveolae. Figure 4B,C shows time-lapse trajectories of PL intensities from a dual-color nanoparticle pair of spots 3 and 5, respectively. Spot 3 shows aspects of caveolae assembly dynamics in which a caveola (green particle) migrates to another caveola (red nanoparticle) within 50 s. During next 50−160 s period, both caveolae are contiguous as reflected in PL increase of green nanoparticle. During this period, the caveolae associate and disassociate multiple times as reflected in PL fluctuations. After 160 s, they bind and co-migrate as evident by correlation of red and green PL intensities. This pattern of dynamic assembly supports our observation that caveolae can associate with one another and form larger structures. Spot 5 shows that red and green nanoparticles were always correlated in PL intensities, indicating that the two particles share the same cellular structure presumably a caveosome.

We observed marked co-localization of caveolin-1 and internalized BSA-coated nanoparticles, indicating that most of the nanoparticles were internalized in caveolae and caveosomes. PEG coating of nanoparticles instead of albumin failed to induce the uptake of nanoparticles. These results show BSA coating is required for the internalization of these particles in endothelial cells, although more studies of BSA specificity in mediating internalization of nanoparticles are needed, such as coating with cationic or denatured BSA to study the role of surface charge in uptake of BSA-coated nanoparticles. The results also are consistent with the key role of the 60 kDa albumin binding protein (gp60) localized in caveolae in a mechanism of caveolae-mediated endocytosis of albumin.[10,11]

We showed that nanoparticle internalization was more efficient for particles smaller than the size of caveolae; the uptake of 20 and 40 nm nanoparticles was 5−10 times greater than 100 nm particles. This result suggests that caveolae size restricts internalization of larger nanoparticles. However, caveolae were still capable of uptake of 100 nm nanoparticles, albeit with reduced efficiency, suggesting that caveolae have the capacity to expand their 10−50 nm sized necks[1] to accommodate the 100 nm particles. Thus, caveola size and shape might be dynamic and dependent on signaling activated by the interaction of albumin-coated particles with the albumin binding proteins expressed in caveolae.[28,30] Size-dependent uptake of nanoparticles also suggests that smaller therapeutic nanoparticles can be more efficiently delivered into cells *via* caveolae. To translate caveolae-mediated nanoparticle delivery to the *in vivo* situation, it will be important to consider cell surface features of the endothelium in the micro-

circulation such as the glycocalyx lining the luminal surface of endothelial cells and the role of circulating albumin concentration in the plasma in interfering with the uptake of the albumin-coated nanoparticles.[4]

We observed that caveolae were able to internalize multiple smaller nanoparticles in single caveolae as measured using counting nanoparticles, suggesting that caveolae are compliant structures with an intrinsic ability to expand their size. A caveola can internalize up to three 20 nm nanoparticles and two 40 nm nanoparticles. This result is consistent with the caveola size and assembly in living endothelial cells measured by a nanoruler made of dual-color nanoparticle pairs. The size and dynamics of caveolae measured using nanoparticles suggest that it is possible using the approach as described to define specific characteristics of these organelles in living endothelial cells.

In summary, we have made three important observations: (1) albumin coating of nanoparticles promotes internalization of nanoparticles in endothelial cells; (2) caveola size is a primary determinant restricting uptake of nanoparticles in endothelial cells; and (3) optical approach using nanoparticles described here allows measurement of caveolae size and assembly dynamics.

MATERIALS AND METHODS

Materials: Carboxylate-modified fluorescence polymer nanoparticles were purchased from Molecular Probes Inc. In our experiment, we used three colors of nanoparticles with different diameters, for example, 24 ± 1 nm (called 20 nm), 36 ± 1 nm (called 40 nm), and 100 ± 1 nm (called 100 nm). In the dual-color experiments, three types of nanoparticles were used, for example, yellow-green (505/515 nm) and red (580/605 nm) or dark red (660/680 nm). Bovine serum albumin (BSA) was purchased from Sigma. Rabbit polyclonal antibody of caveolin-1 was purchased from Santa Cruz Biotechnology Inc. mPEG-NH_2 (polyethylene glycol) was purchased from Laysan Bio Inc., and its molecular weight was 5 kDa. EDC (1-methyl-3-[3-dimethylaminopropyl]carbodiimide hydrochloride) and Sulfo-NHS (*N*-hydroxysulfosuccinimide) were purchased from Pierce Inc. MES ((2-*N*-morpholino)ethanesulfonic acid) was from Fisher Scientific. Centrifuging devices of Nanosep were purchased from Pall Inc.

Synthesis of BSA-Coated Nanoparticles. Figure S1 (in Supporting Information) shows a scheme of synthesis of BSA-coated nanoparticles. We coated a full monolayer of BSA molecules on fluorescent polymer nanoparticles with diameters of 20, 40, or 100 nm *via* covalent bonds between nanoparticle surfaces and BSA molecules. To activate COOH groups on fluorescent polymer nanoparticles, for example, in case of 40 nm particles, 0.1 mL of original particle solution in 0.9 mL of MES buffer (50 mM, pH = 6) is mixed with 25 μL of EDC (80 mg/mL) and 25 μL of Sulfo-NHS (160 mg/mL) for reaction of 15 min. The mixture was centrifuged using Nanosep-50K (OD50C33) (Pall Inc.) three times and was dissolved in PBS buffer (pH = 7.4). After activation of nanoparticles, we added a defined amount of BSA solution to the activated particle solution and allowed them to react for 2 h in room temperature. We separated free BSA molecules from BSA-coated nanoparticles using Nanosep-300K centrifuge devices (OD300C33) three times. We used the same method coating mPEG-NH_2 molecules to nanoparticles. To determine the importance of BSA ligands for nanoparticle internalization, we added the same amount of BSA molecules per nanoparticle for each size of nanoparticles and allowed them to react for 2 h. After the reaction, we added mPEG-NH_2 into the BSA-coated nanoparticle solution to occupy the empty area to which BSA does not bind. Coating of mPEG-NH_2 will reduce nonspecific uptake of nanoparticles. BSA-coated nanoparticles were characterized by absorption spectra using Carey 300 Bio. BSA molecules were conjugated to nanoparticle surfaces as evident of BSA absorption at 280 nm (Figure S2). On the basis of the absorption coefficient of BSA, we estimated the number of BSA per particle, as 110 ± 30 BSA for 20 nm particles, 300 ± 60 BSA for 40 nm particles, and 2000 ± 200 BSA for 100 nm particles.

We also conjugated Alexa-488 labeled BSA (green emission) to red fluorescent nanoparticles. Simultaneous detection of a double-labeled nanoparticle suggests that BSA was conjugated to nanoparticle surfaces because the nanoparticles and Alexa-488 always moved together in suspension (Figure S3). Absorption spectrum and simultaneous dual-color imaging indicate BSA was conjugated to the fluorescent nanoparticles.

Endothelial Cells. Endothelial cells were grown in MCDB131 medium supplemented with endothelial cell growth media (L-glutamine, penicillin, EFG, hydrocortisone) and 10% FBS. Passage 4 or 5 of cultured cells was used in all experiments. Bovine lung microvessel endothelial cells (BLMVEC) purchased from VecTec Rensselaer, NY, were used in all experiments unless otherwise stated.

Endothelial Uptake of BSA-Coated Nanoparticles. BLMVECs grown to confluence on coverslips were washed and incubated with 5 mM Hepes/Hank's balanced salt solution (HBSS, pH 7.4) overnight at 37 °C and 5% CO_2. We incubated BSA-coated nanoparticles at the same concentration of nanoparticles with different sizes in 5 mM Hepes/HBSS (at 0.02−0.12 nM of nanoparticles) with cells for different periods. We stopped the uptake of nanoparticles by putting them on ice and washing them with cold NaAc buffer (pH 4.5) to wash out the nanoparticles that did not internalize into cells. Cells were fixed in 4% paraformaldehyde (PFA) in PBS buffer in the room temperature for 20 min and washed by PBS and finally were mounted on glass slides. We imaged samples using a 20× objective and Axiocam from Zeiss with suitable fluorescence filters and measured integrated PL using ImageJ and averaged several locations on samples (Figure S5). Figure S4 is a *YZ* projection of 3D confocal fluorescence images of nanoparticle uptake by cells, showing the fast and size-dependent uptake of BSA-coated nanoparticles.

Co-localization of Nanoparticles with Caveolae. For co-localization of BSA nanoparticles with caveolae, BLMVECs grown to confluence on coverslips were washed and incubated with 5 mM Hepes/Hank's balanced salt solution (HBSS, pH 7.4) overnight at 37 °C and 5% of CO_2. After uptake of nanoparticles by cells and fixture, cells were permeabilized in blocking buffer (PBS containing 3% (w/v) BSA, 5% goat serum and 0.5% Triton-100) for 20 min. Cells were then incubated with primary antibodies (polyclonal rabbit anticaveolin-1) for overnight at 4 °C or 2 h in the room temperature and secondary antibodies labeled by fluorescence dyes (goat anti-rabbit IgG) for 20 min. Cells were washed by PBS and mounted on a glass slide. Images were taken using a 100× oil immersion objective in confocal scanning microscope (LSM 510 meta).

Size Measurement of Caveolae and Caveosomes. A mixture of dual-color nanoparticles was incubated with cells, and the cells were fixed by 4% paraformaldehyde (PFA) in PBS buffer. We imaged using a confocal microscope and measured the distance between fluorescent spot centers for green and red nanoparticles.

Live Cell Imaging. BLMVEC was grown on glass coverslips and overnight incubated in 5 mM Hepes in HBSS. During imaging, cells were maintained in 5 mM Hepes in HBSS and at 37 °C. For simultaneous dual-color imaging of tracking nanoparticles, we set up two laser beams (488 and 633 nm) collimated to excite cells and simultaneously obtained images on two separate chan-

nels with suitable fluorescent filters at a fast scanning speed. Each frame took 1−2 s to record.

Image Analysis and Histogram Fitting. All image analysis was used by ImageJ. For PL intensity distribution of nanoparticles internalized in cells, only spots of the size close to optical diffraction limit were considered. PL intensity was calculated by averaging intensity of circular ROI of 8−10 pixels in radius drawn around fluorescent spots and by subtracting background. Obtained histograms (*e.g.*, Figure 2D) were fitted using the function consisting of 1−4 Gaussian profiles in Origin based on the equation

$$F(n) = \sum_{n=0} A_n e^{-(I+nq)^2/2n\sigma^2}$$

Where $F(n)$ is the nth Gaussian profile at a given PL intensity I, A_n is the amplitude of nth peak, σ is the variance of intensity of an individual Gaussian profile, and q is the intensity of an individual quantum. In the histogram of vesicular size in dual-color imaging, we also fit them by Gaussian profiles using Origin software.

Acknowledgment. We thank Dr. J. Lippincott-Schwartz for valuable discussion and Y.B. Wu for help in cell culture. This work was supported by NIH grants (P01HL060678, P01HL077806, and R01HL045638).

Supporting Information Available: Synthesis of conjugated nanoparticles and movies of nanoparticle trafficking in live cells. This material is available free of charge *via* the Internet at http://pubs.acs.org.

REFERENCES AND NOTES

1. Predescu, S. A.; Predescu, D. N.; Malik, A. B. Molecular Determinants of Endothelial Transcytosis and Their Role in Endothelial Permeability. *Am. J. Physiol. Lung Cell Mol. Physiol.* **2007**, *293*, L823–L842.
2. McIntosh, D. P.; Tan, X. Y.; Oh, P.; Schnitzer, J. E. Targeting Endothelium and Its Dynamic Caveolae for Tissue-Specific Transcytosis *In Vivo*: A Pathway to Overcome Cell Barriers to Drug and Gene Delivery. *Proc. Natl. Acad. Sci. U.S.A.* **2002**, *99*, 1996–2001.
3. Parton, R. G.; K.; Simons, K. The Multiple Faces of Caveolae. *Nat. Rev. Mol. Cell Biol.* **2007**, *8*, 185–194.
4. Mehta, D.; Malik, A. B. Signaling Mechanisms Regulating Endothelial Permeability. *Physiol. Rev.* **2006**, *86*, 279–367.
5. Pelkmans, L. Secrets of Caveolae- and Lipid Raft-Mediated Endocytosis Revealed by Mammalian Viruses. *Biochim. Biophys. Acta* **2005**, *1746*, 295–304.
6. Nabi, I. R.; Le, P. U. Caveolae/Raft-Dependent Endocytosis. *J. Cell. Biol.* **2003**, *161*, 673–677.
7. Nichols, B. Caveosomes and Endocytosis of Lipid Rafts. *J. Cell. Sci.* **2003**, *116*, 4707–4714.
8. Oh, P.; Borgstrom, P.; Witkiewicz, H.; Li, Y.; Borgstrom, B. J.; Chrastina, A.; Iwata, K.; Zinn, K. R.; Baldwin, R.; Testa, J. E.; Schnitzer, J. E. Live Dynamic Imaging of Caveolae Pumping Targeted Antibody Rapidly and Specifically across Endothelium in the Lung. *Nat. Biotechnol.* **2007**, *25*, 327–337.
9. Tiruppathi, C.; Naqvi, T.; Wu, Y.; Vogel, S. M.; Minshall, R. D.; Malik, A. B. Albumin Mediates the Transcytosis of Myeloperoxidase by Means of Caveolae in Endothelial Cells. *Proc. Natl. Acad. Sci. U.S.A.* **2004**, *101*, 7699–7704.
10. Shajahan, A. N.; Timblin, B. K.; Sandoval, R.; Tiruppathi, C.; Malik, A. B.; Minshall, R. D. Role of Src-Induced Dynamin-2 Phosphorylation in Caveolae-Mediated Endocytosis in Endothelial Cells. *J. Biol. Chem.* **2004**, *279*, 20392–20400.
11. Minshall, R. D.; Sessa, W. C.; Stan, R. V.; Anderson, R. G.; Malik, A. B. Caveolin Regulation of Endothelial Function. *Am. J. Physiol. Lung Cell Mol. Physiol.* **2003**, *285*, L1179–L1183.
12. Pelkmans, L.; Zerial, M. Kinase-Regulated Quantal Assemblies and Kiss-and-Run Recycling of Caveolae. *Nature* **2005**, *436*, 128–133.
13. Betzig, E.; Patterson, G. H.; Sougrat, R.; Lindwasser, O. W.; Olenych, S.; Bonifacino, J. S.; Davidson, M. W.; Lippincott-Schwartz, J.; Hess, H. F. Imaging Intracellular Fluorescent Proteins at Nanometer Resolution. *Science* **2006**, *313*, 1642–1645.
14. Wilig, K. I.; Rizzoli, S. O.; Westphal, V.; Jahn, R.; Hell, S. W. STED Microscopy Reveals that Synaptotagmin Remains Clustered after Synaptic Vesicle Exocytosis. *Nature* **2006**, *440*, 935–939.
15. Kittel, R. J.; Wichmann, C.; Rases, T. M.; Fouquet, W.; Schimdt, M.; Schimd, A.; Wagh, S. A.; Pawlu, C.; Kellner, R.; Willig, K. I.; Hell, S. T.; Buchner, E.; Heckmann, M.; Sigrist, S. J. Bruchpilot Promotes Active Zone Assembly, Ca^{2+} Channel Clustering, and Vesicle Release. *Science* **2006**, *312*, 1051–1054.
16. Qu, X.; Wu, D.; Metes, L.; Scherer, N. F. Nanometer-Localized Multiple Single-Molecule Fluorescence Microscopy. *Proc. Natl. Acad. Sci. U.S.A.* **2004**, *101*, 11298–11303.
17. Ram, S.; Ward, E. S.; Ober, R. J. Beyond Rayleigh's Criterion: A Resolution Measure with Application to Single-Molecule Microscopy. *Proc. Natl. Acad. Sci. U.S.A.* **2006**, *103*, 4457–4462.
18. Yildiz, A.; Selvin, P. R. Fluorescence Imaging with One Nanometer Accuracy: Application to Molecular Motors. *Acc. Chem. Res.* **2005**, *38*, 574–582.
19. Huang, B.; Wang, W.; Bates, M.; Zhuang, X. Three-Dimensional Super-Resolution Imaging by Stochastic Optical Reconstruction Microscopy. *Science* **2008**, *319*, 810–813.
20. *Biofunctionalization of Nanomaterials*; Kumar, C., Ed.; Wiley-VCH: Weinheim, Germany, 2005.
21. Niemeyer, C. M. Nanoparticles, Proteins, and Nucleic Acids: Biotechnology Meets Materials Science. *Angew. Chem., Int. Ed.* **2001**, *40*, 4128–4158.
22. Chan, W. C. W.; Maxwell, D. J.; Gao, X. H.; Beiley, R. E.; Han, M. Y.; Nie, S. M. Luminescent Quantum Dots for Multiplexed Biological Detection and Imaging. *Curr. Opin. Biotechnol.* **2002**, *13*, 40–46.
23. Alivisatos, A. P. The Use of Nanocrystals in Biological Detection. *Nat. Biotechnol.* **2004**, *22*, 47–52.
24. Ding, B.-S.; Dziubla, T.; Shuvaev, V. V.; Muro, S.; Muzykantov, V. R. Advanced Drug Delivery Systems That Target the Vascular Endothelium. *Mol. Interv.* **2006**, *6*, 98–112.
25. Nie, S.; Xing, S.; Kim, G. J.; Simons, J. W. Nanotechnology Applications in Cancer. *Annu. Rev. Biomed. Eng.* **2007**, *9*, 256–288.
26. Liu, Z.; Cai, W.; He, L.; Nakayama, N.; Chen, K.; Sun, X.; Chen, X.; Dai, H. *In Vivo* Biodistribution and Highly Efficient Tumor Targeting of Carbon Nanotubes in Mice. *Nat. Nanotechnol.* **2007**, *2*, 47–52.
27. Vogel, S. M.; Minshall, R. D.; Pilipovic, M.; Tiruppathi, C.; Malik, A. B. Albumin Uptake and Transcytosis in Endothelial Cells *In Vivo* Induced by Albumin-Binding Protein. *Am. J. Physiol. Lung Cell Mol. Physiol.* **2001**, *281*, L1512–L1522.
28. John, T. A.; Vogel, S. M.; Tiruppathi, C.; Malik, A. B.; Minshall, R. D. Quantitative Analysis of Albumin Uptake and Transport in the Rat Microvessel Endothelial Monolayer. *Am. J. Phyisol. Lung Cell Mol. Physiol.* **2003**, *284*, L187–L196.
29. Pelkmans, L.; Kartenbeck, J.; Helenius, A. Caveolar Endocytosis of Simian Virus 40 Reveals a New Two-Step Vesicular-Transport Pathway to the ER. *Nat. Cell Biol.* **2001**, *3*, 473–483.
30. Minshall, R. D.; Tiruppathi, C.; Vogel, S. M.; Niles, W. D.; Gilchrist, A.; Hamm, H. E.; Malik, A. B. Endothelial Cell-Surface gp60 Activates Vesicle Formation and Trafficking a G(i)-Coupled Src Kinases Signaling Pathway. *J. Cell. Biol.* **2000**, *150*, 1057–1070.